

# ENTROPIC AND MULTIFRACTAL ANALYSIS OF DISORDERED MORPHOLOGIES

A. BEGHDADI

*L.P.M.T.M., C.N.R.S., Institut Galilée, Université Paris Nord,  
93430 Villetaneuse, France*

C. ANDRAUD, J. LAFAIT and J. PEIRO

*Laboratoire d'Optique des Solides, Université Pierre et Marie Curie,  
C.N.R.S., 4, Place Jussieu, 75252 Paris Cedex 05, France*

M. PERREAU

*L.E.M., C.N.R.S./O.N.E.R.A., BP 102, 92322 Châtillon Cedex, France*

## Abstract

We propose the configuration entropy as an efficient tool of characterization of the disorder of random morphologies and as a pertinent morphological parameter for describing the optical properties. When increasing the size of observation of an image, it undergoes a maximum at a characteristic length which is the optimum length at which the image must be observed to get the maximum information. When applied to computer simulated images, the configuration entropy is more powerful, less ambiguous and less sensitive to the finite size of images than the generalized fractal dimension.

## 1. INTRODUCTION

Morphology governs all the physical properties of heterogeneous materials. This is particularly the case for the optical properties of granular metal films.<sup>1</sup> The problem of relating quantitatively the morphology and the optical properties under the form of parameters in a model is not yet solved. Some attempts were made with success to explain the characteristic extra absorption occurring around the percolation in these granular metals.<sup>2,3</sup>

They use characteristic parameters involved in scaling laws at percolation: metal fraction  $p$ , correlation length  $\xi$ , critical exponents, fractal dimension  $D_F$  of the infinite cluster, and the fractal dimension of its backbone which can be extracted from a statistical geometrical analysis of the morphology.

We have, however, some examples of granular metal layers deposited under different conditions (rate of deposition, temperature of the substrate, ...) which exhibit notably different optical properties, although having the same metal fraction, and fractal dimension and a flat multifractal spectrum. These parameters: metal fraction, fractal dimension (and doubtless multifractal spectrum) are thus not enough to describe the optical properties. This is the reason why we have explored another way of description of the disorder related to thermodynamical concepts and theory of information: the configuration entropy.<sup>4</sup>

The entropy of a physical system has often been described as a measure of randomness in the structure of the system. Moreover, the entropy measures the lack of information<sup>5</sup> or the degree of uncertainty in the realization of an event in a given experiment. Since the pioneer work of Shannon<sup>6</sup> in information theory, the entropy concept is widely used in many fields.<sup>7-9</sup>

## 2. CONFIGURATION ENTROPY

Shannon defined the entropy of a system as a function of the probability of occurrence of different states of the system. If a system has  $n$  different possible states with probability of occurrence  $p_i$ ,  $i = 1, 2, \dots, n$ , then the gain in information from the occurrence of the event  $i$  is defined as:

$$I_i = \ln \frac{1}{p_i} \quad (1)$$

The expected value of such a gain in information is defined as the entropy  $H$  of the system:

$$H = \sum_{i=1}^n p_i I_i \quad \text{or} \quad H = - \sum_{i=1}^n p_i \ln p_i \quad (2)$$

It can be noted that since  $H$  is a function of the probability  $p_i$  associated with a given source of symbols or a random variable, one can derive an entropy for each defined source. In the present study, the system is a binary image representing a two-phase material and the elementary source symbol is the pixel intensity which has two possible values 1 or 0 ("black" and "white" representation).

The image is analyzed through an elementary sliding cell of size  $l \times l$ . For a given position of the cell  $C_{ij}$ , we count the number of active pixels (pixels having value 1) contained in  $C_{ij}$ . Once the whole image is examined, we compute  $N_k(l)$ : number of cells containing  $k$  active pixels, and  $N(l)$ : total number of visited cells. Thus, the probability associated with the state of the cell is defined as follows:

$$P_k(l) = \frac{N_k(l)}{N(l)} \quad (3)$$

The corresponding entropy is:

$$H(l) = - \sum_{k=0}^{l^2} p_k(l) \ln p_k(l) \quad (4)$$

Obviously,  $H$  is a measure of the degree of uncertainty in the realization of a given state of the cell of size  $l \times l$ . Using the Lagrange multiplier method, one can easily show that  $H(l)$  is maximized under the constraint:

$$\sum_{k=0}^{l^2} p_k(l) = 1 \quad (5)$$

when the different cell configurations are equally probable, i.e., when

$$p_k(l) = \frac{1}{l^2 + 1} \quad (6)$$

for every  $k$ . To examine the image structure at different length scale, the cell size is increased from  $l = 1$  to  $l = L/2$ . To compare the entropy values obtained for different  $l$  values one has to normalise  $H(l)$ . We thus compute for each  $l$  value the normalized entropy defined by:

$$H^*(l) = \frac{H(l)}{H_{\max}(l)} \quad (7)$$

where

$$H_{\max}(l) = \ln(l^2 + 1) \quad (8)$$

$H^*(l)$  undergoes a maximum at a characteristic size  $l^*$  that we call the entropy optimum length. The box of size  $l^* \times l^*$  presents a maximum of disorder and is the optimum area at which the image must be observed and eventually characterized with the aim of optical studies. We have also proved that the configuration entropy increases with the cluster ramification and the system lacunarity.

### 3. FRACTALITY, MULTIFRACTALITY AND ENTROPY

It has been shown by many authors that many physical systems consisting of objects having complex shape can be described in terms of fractal geometry.<sup>10-14</sup> Since the pioneer works of Mandelbrot, the characterization of random or statistical fractals has been increasingly developed and refined with the introduction of multifractal formalism.<sup>15-19</sup>

The concept of multifractal is related to the properties of the distribution of the mass associated with a measure defined on the object.<sup>17-20</sup> The object can be regarded in this approach as a family of different homogeneous fractal sets on which the measure has a given singularity. To analyze the multifractality of a given object, the support of the measure is covered with boxes of size  $l \times l$  and the probability  $p_i(l)$ , which is the integrated measure, is computed in each box. The generalized dimension defined by:

$$D_q = \frac{1}{q-1} \lim_{l \rightarrow 0} \frac{\ln \sum_i p_i^q(l)}{\ln l} \quad (9)$$

characterizes the non-uniformity of the measure.<sup>19</sup>

In practice, Eq. (9) cannot be directly used to compute the generalized dimension. Indeed, the exact value of the generalized dimension is only obtained when the box size tends to zero. Vicsek et al.<sup>20-22</sup> proposed practical methods to compute the generalized dimension. They must assume the box size to be much greater than the smallest elementary cell in the

system and much smaller than the system size. They have thus shown that the standard methods for determining fractal dimensions have to be applied with some caution. The box counting method is only efficient when the cluster size is large enough and in the sand box method the results depend on the selected centers of the analysis boxes.

Recently, Blacher et al.<sup>23</sup> used the approach of Chhabra et al.<sup>19</sup> to compute the Hausdorff dimension of simulated clusters. Chhabra et al. define a family of normalized measures as follows:

$$\mu_i(q, l) = \frac{(p_i(l))^q}{\sum_j (p_j(l))^q} \quad (10)$$

Thus, the Hausdorff dimension is given by:

$$f(q) = \lim_{l \rightarrow 0} \frac{\sum_i \mu_i(q, l) \ln \mu_i(q, l)}{\ln l} \quad (11)$$

It can be noted that for  $q = 1$ , the numerator is a quantity similar to the one used in our approach [Eq. (4)], namely, the configuration entropy. For this reason, the corresponding dimension  $D_1$  is called the information dimension. In our approach, the maximum value of entropy allows the measurement of the optimum box size corresponding to the highest degree of disorder in the system under observation. In the multifractal analysis, the maximum value of  $f(q)$ , for  $q = 0$ , gives the Hausdorff dimension of the object of the measure, namely  $D_0$ .

The main difficulty in using the multifractal formalism lies in the fact that the ideal limit  $l = 0$  cannot be reached in practice. Furthermore, one usually needs only a very limited subset of the spectrum  $f(q)$  in order to describe the important properties of the associated measure. Only the cases  $q = 0$ ,  $q = 1$  and  $q = 2$  could be unambiguously relied on to make a physical interpretation of the system. Merits and limitations of the multifractal analysis have been discussed by Aharony.<sup>24</sup> In the same way, Chhabra et al.<sup>19</sup> pointed out the risks in the estimation of the Hausdorff dimension and cited different sources of errors in some physical cases. The difficulties arising in practice are due to the fact that the relevant quantities used in the multifractal concept are estimated asymptotically. In our approach, however, there is no ambiguity in the computation of our relevant quantities. Moreover, the measure of the correlation length  $\xi$  marking the limit of the scaling behavior is determined with poor accuracy using the fractal formalism.<sup>25</sup> On the other hand, the optimum length characterizing the maximum of disorder is unambiguously determined with our entropic approach.

The main purpose of the present study is not to compare in detail our approach to the fractal and multifractal analysis but to propose another powerful tool to measure the disorder in systems having a complex structure, and to show that, in a usual case, this tool is efficient and less ambiguous than these analysis. Furthermore, the characteristic length defined through the entropy concept could be used for optical characterization of two-phase materials.

#### 4. APPLICATION TO RANDOM MORPHOLOGIES

We now demonstrate the efficiency of the configuration entropy as compared to the fractal dimension in two limit cases:



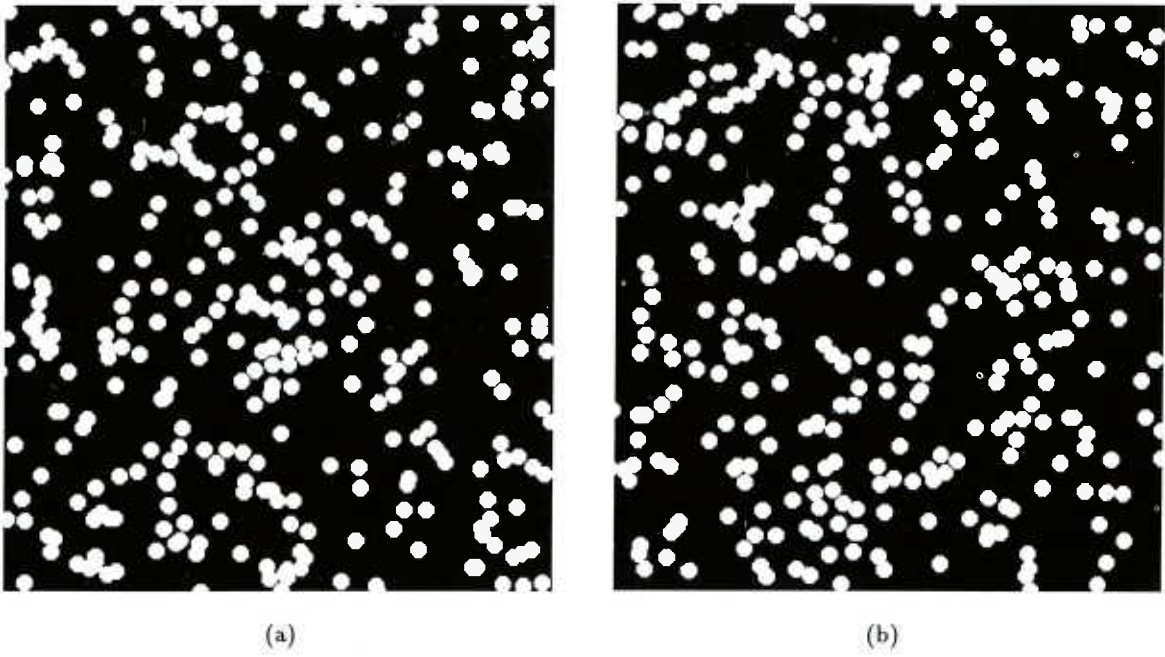


Fig. 1 Computer simulated random morphologies obtained by random throws of overlapping disks of size 11 pixels: (a) First throw; (b) Second throw. (Image size 400 \* 400 pixels.)

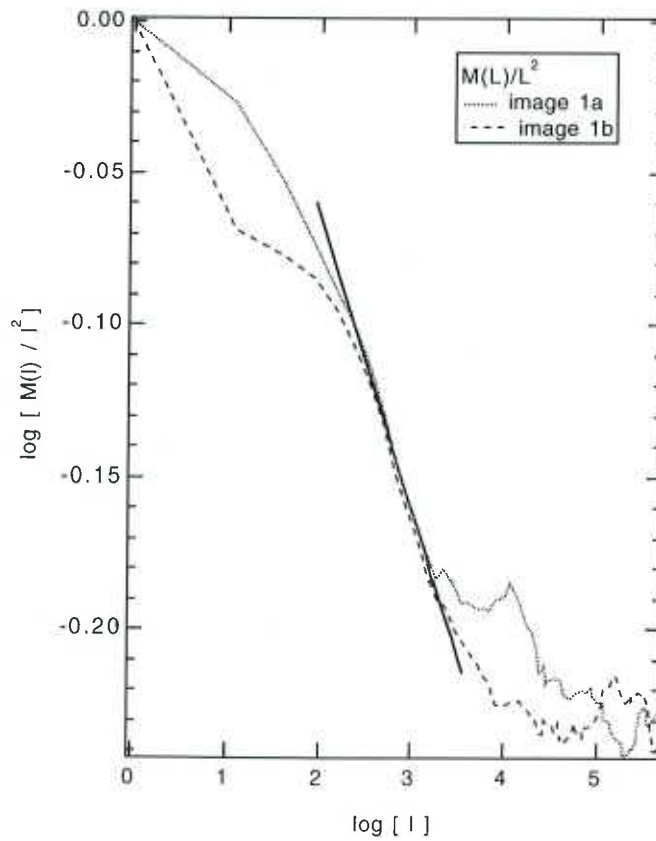


Fig. 2 Log-log plot of the black mass contained in a square of size  $l$  in images 1(a) and 1(b) (sand box method). The linear regression in the scaling domain is indicated. Slope  $\approx -0.1$ ;  $D_F \approx 1.9$ .

(1) Two very close images of the same size (400\*400) composed of penetrating disks of the same size and the same concentration 0.20. The images differ only in the fact that they have been obtained after two different sequences of random trials. They can hardly be differentiated by visual observation [Figs. 1(a) and 1(b)]. The fractal dimension of the complementary set of the disks in the image is determined by the classical sand box method.<sup>20,21</sup> The scaling region clearly shows up in Fig. 2. The fractal dimension  $D_F$  thus deduced is 1.90 for both images. The finite size of the images and the lacunarity reduce the accuracy of the linear regression in the scaling region. For the same reasons, the average behavior following the scaling region merges into fluctuations. It is thus impossible to correctly evaluate the correlation length marking the transition between these two regimes. We then used the sand box method for the calculation of the generalized fractal dimension of order  $q$ :  $D_q$ , related to the multifractal spectrum via Legendre transform.<sup>20,21</sup> Both images do not present any multifractality, the straight line characterizing the different orders being indiscernible. The classical geometrical parameters of both images are thus equal.

The configuration entropy as calculated by our method presented above, exhibits for its parts some differences when applied to these images (Fig. 3). First, the two entropy curves are clearly discernible; second, both curves undergo a maximum  $H_{\max}^*$  for an optimum length  $l_0$ . The small differences in these values, as shown in Fig. 3, are nevertheless significant

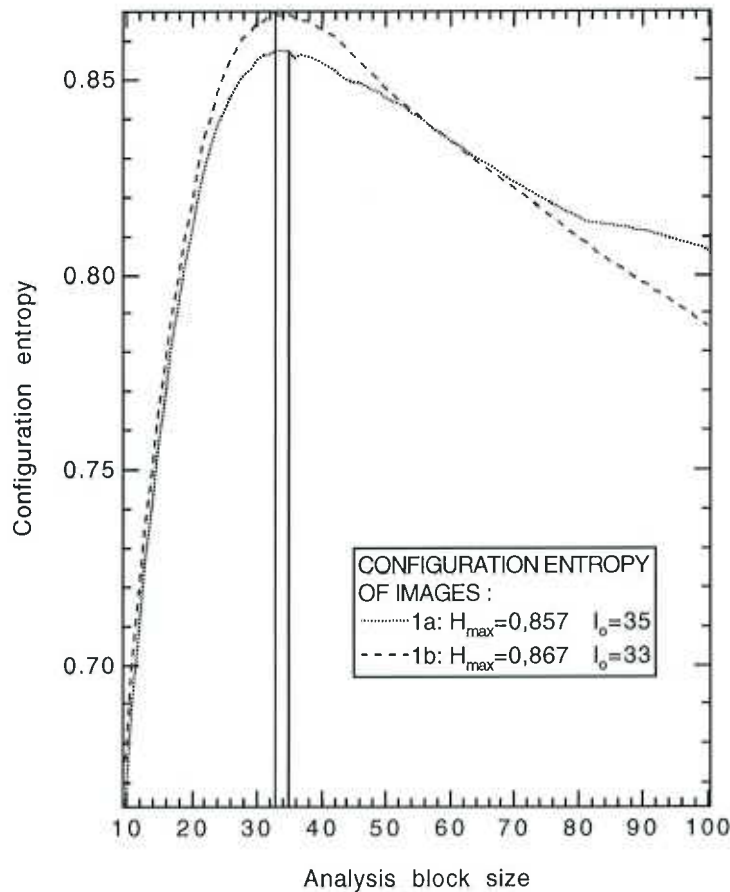
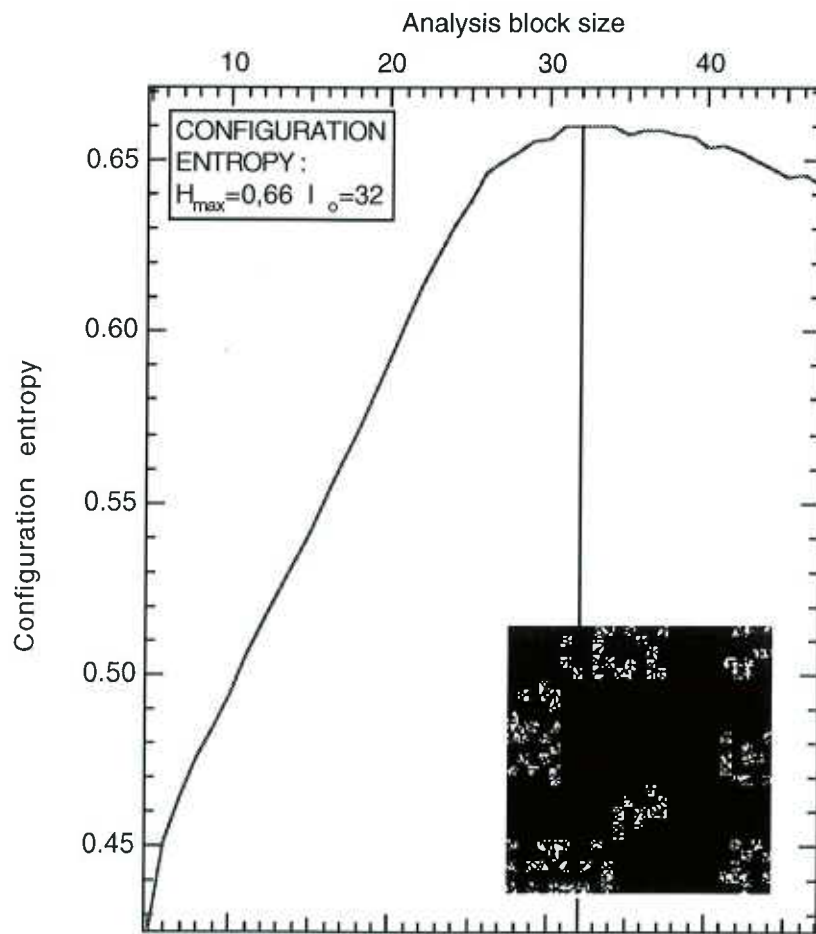


Fig. 3 Configuration entropy of images 1(a) and 1(b). Entropy maxima and related optimal lengths are indicated.

because of the high accuracy of their determination. It can be concluded that, in this limit case of quasi similar images, the configuration entropy succeeds in emphasizing an undeniable difference whereas other classical tools fail.

(2) We now envisage the analytical generation of two images for which one knows exactly the fractal dimension. These images are square Sierpinski carpets from which some pixels have been randomly removed at each step of iteration.  $n$ , being the size of the starting pattern,  $p$ , the number of blocks to remain in this starting pattern and  $k$ , the number of iterations: the size of the image is  $n^k * n^k$  and its fractal dimension is  $D_F = \log(p)/\log(n)$ . Both images have the same concentration: 0.23 and their fractal dimension is:  $D_{Fa} = 1.43$ ;  $D_{Fb} = 1.73$ .

Because of the low number of iterations, it is impossible to determine the fractal dimension by the sand box method. Nevertheless, the configuration entropy gives non-ambiguous results as shown in Figs. 4(a) and 4(b).

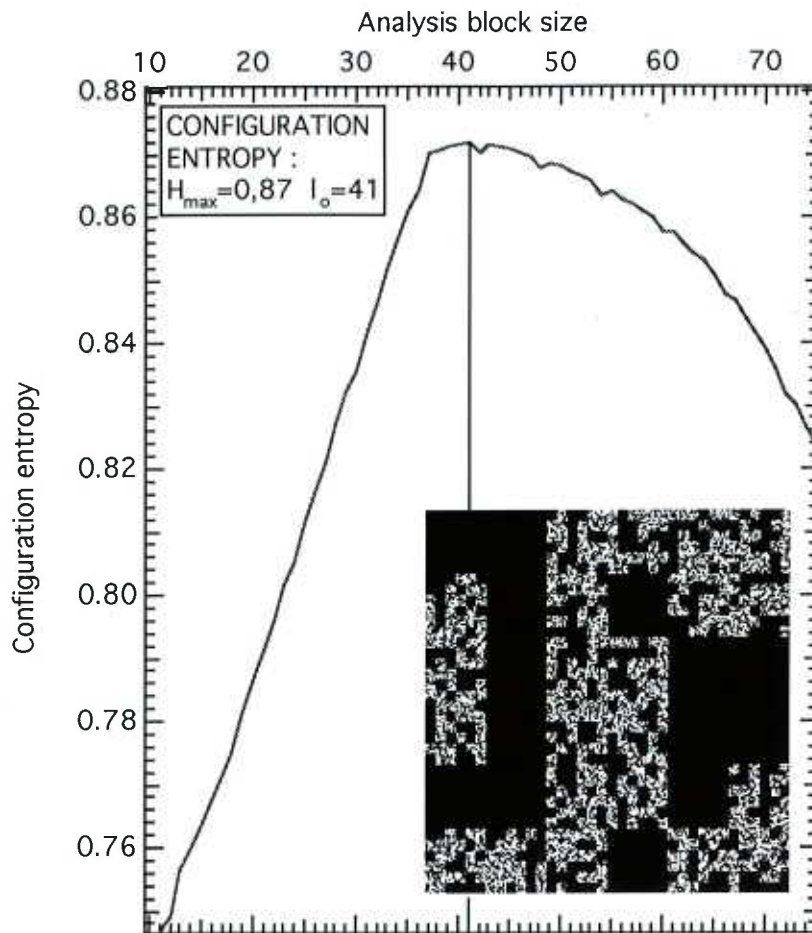


(a)

**Fig. 4** Computer simulated morphologies obtained by randomly removing sites on a square Sierpinski carpet with starting pattern size  $n$ , number of remaining sites in this pattern  $p$ , number of iterations  $k$ , and the corresponding entropy.

(a)  $n = 5$   $p = 10$   $k = 3$  size =  $125 * 125$  pixels  $D_{Fa} = 1.43$

(b)  $n = 6$   $p = 22$   $k = 3$  size =  $216 * 216$  pixels  $D_{Fb} = 1.73$



(b)

Fig. 4 (Continued)

In these two extreme examples, the classical geometrical parameters are either indiscernible or cannot be determined geometrically, whereas the configuration entropy is always unambiguous: well defined distinct maxima and of different optimum lengths.

## 5. CONCLUSION

We have shown in these limit cases, that the configuration entropy is a powerful tool well adapted to the characterization of disorder and able to separate out very close morphologies when fractal and multifractal analysis fails. In any case, this tool never gives ambiguous results and is less sensitive to the finite size of images, in contrast to fractal and multifractal analysis. The next but difficult step will be to incorporate this parameter in a quantitative model of the optical properties of these random morphologies.

## REFERENCES

1. P. Gadenne, A. Beghdadi and J. Lafait, *Optics Commun.* **65**, 17 (1988).
2. Y. Yagil, M. Yosefin, D. J. Bergman, G. Deutscher and P. Gadenne, *Phys. Rev.* **B43**, 1342 (1991).



3. T. Robin and B. Souillard, *Physica* **A193**, 79 (1993).
4. H. O. Peitgen and D. Saupe, *The Science of Fractal Images* (Berlin, 1988).
5. L. Brillouin, *Science an Information Theory* (Academic Press Inc., New York, 1956).
6. C. E. Shannon, *Bell. Syst. Tech. J.* **210**, 623 (1948).
7. B. R. Frieden, *J. Opt. Soc. Amer.* **62**, 511 (1972).
8. S. F. Gull and T. J. Newton, *Applied Optics* **25**, 156 (1986).
9. A. Mohammad-Djafari and G. Demoment, *Applied Optics* **26**, 1745 (1987).
10. B. B. Mandelbrot, *The Fractal Geometry of Nature* (W. H. Freeman, New York, 1982).
11. R. F. Voss, R. B. Laibowitz and E. I. Alessandrini, *Phys. Rev. Lett.* **49**(19), 1441 (1982).
12. R. Orbach, *Science* **231**, 814 (1986).
13. J. F. Gouyet, *Physique et structures fractales* (Masson, Paris, 1992).
14. L. Pietronero, *Physica* **A144**, 257 (1987).
15. B. B. Mandelbrot, *J. Fluid. Mech.* **62**, 331 (1974).
16. G. Paladin and A. Vulpiani, *Phys. Rep.* **156**, 147 (1987).
17. M. H. Jensen, L. P. Kadanoff and A. Libchaber, *Phys. Rev. Lett.* **55**, 2798 (1985).
18. T. C. Halsey, M. H. Jensen, L. P. Kadanoff, I. Procaccia and B. I. Shraiman, *Phys. Rev.* **A33**, 1141 (1986).
19. A. B. Chhabra, C. Meneveau, R. V. Jensen and K. R. Sreenivasan, *Phys. Rev.* **A40**, 5284 (1989).
20. T. Vicsek, *Fractal Growth Phenomena*, 2nd ed. (World Scientific Publishing Co, Singapore, 1992).
21. T. Vicsek, *Physica* **A168**, 490 (1990).
22. T. Tel, A. Fülöp and T. Vicsek, *Physica* **A159**, 155 (1989).
23. S. Blacher, F. Brouers and R. Van Dyck, to appear in *Physica A* (1993).
24. A. Aharony, *Physica* **A168**, 479 (1990).
25. A. Beghdadi, J. Lafait, P. Gadenne, A. Constans and O. Bouet, *Acta Stereol* **6/III**, 809 (1987).